Noble Metal Wax Hydrocracking Catalysts Supported on High-Siliceous Alumina

ARTICLE *in* INDUSTRIAL & ENGINEERING CHEMISTRY RESEARCH · APRIL 2007

Impact Factor: 2.59 · DOI: 10.1021/ie0700922

1 AUTHOR:

Dieter Leckel
Suid Afrikaanse Steenkool en Olie
23 PUBLICATIONS **408** CITATIONS

SEE PROFILE

Noble Metal Wax Hydrocracking Catalysts Supported on High-Siliceous Alumina

Dieter Leckel[†]

Fischer-Tropsch Refinery Catalysis, Sasol Technology Research and Development, P.O. Box 1, Sasolburg 1947, South Africa

Amorphous silica−aluminas formed by alumina obtained from the sililation of aluminum alkoxides with othosicilic acid were used as support material for the preparation of bifunctional hydrocracking catalysts. Brønsted acidity, which was observed for the support with 40% silica (Siral40), was absent in the material with 75% silica (Siral75). Impregnation with Pt or Pt and W, however, generated not only Brønsted acidity on Siral75 but also resulted in a higher platinum dispersion relative to Siral40. The PtW75 catalyst showed the behavior of *ideal hydrocracking* during hydrocracking of *n*-hexadecane. A high-quality diesel was obtained with high selectivity even at conversion levels above 90% during hydrocracking of Fischer−Tropsch wax. The performance of the PtW75 catalyst proved to be comparable or even better than the commercial catalyst tested.

Introduction

Hydrocracking of low-temperature Fischer−Tropsch (LTFT) waxes is to date carried out with a variety of catalysts such as sulfided base-metal catalysts based on amorphous silica−alumina supports,[1] platinum-loaded sulfated or tungstated zirconia supported catalysts,[2] or noble metal promoted silica−alumina catalysts.[3,4] The common feature of all the catalysts employed is the bifunctional nature comprised of a dehydrogenation−hydrogenation metal component dispersed on acidic amorphous silica−alumina.[5,6]

For the preparation of silica−alumina containing acid sites two major methods are employed. One of them uses the cohydrolyses of silica and alumina sources which results in matter commonly referred to as *silica−alumina*,[7] while the other one uses *silication*[8] of alumina, resulting in material which can be attributed to as *silicated* alumina[9] or aluminosilicates. The preparation of silicated alumina, referred to as *stabilized* aluminas, was already described in 1977, when Snamprogetti was granted patents[10] on the preparation of aluminas having improved mechanical and thermal properties. Esters and salts of orthosicilic acids or alkyl orthosilicates were thereby used as silicon compounds for impregnating aluminum oxides (preferably γ-alumina). The stabilized aluminas were used for the skeletal isomerization of alkenes, more precisely, butenes and pentenes, to form isoalkenes.

Silicated aluminas prepared from tetraethoxysilane are described by Nilsen et al.,[8] who investigated the material as catalyst for the skeletal isomerization of butenes. Niwa et al.[11] deposited a thin layer of silica on alumina and characterized the surface acidity together with catalytic activity for test reactions such as cumene cracking, isomerization of 1-butene, and alcohol dehydration. The lack of strong Brønsted acidity of the silanols attached to alumina was reported and the acid strength of the assumed −Al−O−Si−OH species was considered to be relatively weak. Thus, silication of alumina lead to weak Brønsted acidity; however, the weakly acidic protons were sufficient for carbenium ion formation and isomerization.

A comprehensive surface acidity study was done by Daniell et al.[12] on silica−aluminas commercially available as *Siral* materials using FTIR spectroscopy and CO as probe molecule. These silica−aluminas were prepared by modification of γ-alumina with silica according to a patented procedure,[13] involving the hydrolysis of a solution of aluminum hexanolate followed by mixing the filtered alumina suspension with a solution of orthosilicic acid. By variation of the amount of orthosilicic acid used, samples containing between 1.5 and 90 mass % silica can be prepared. It was reported in the study that Lewis and Brønsted acidity increased with silica loading and peaked at a silica loading of 40 mass % for the Siral40 material (the number indicates thereby the SiO_2 content of the silicated alumina material). Higher silica contents (above 40% SiO_2) resulted in a progressive coverage of the alumina material by silica, whereby materials with 70 mass % silica or more (such as Siral70) showed no evidence for enhanced Brønsted acidity according to XPS measurements.[12]

In this paper we will show that a silica−alumina with 75% silica (Siral75) that was reported to have practically no Brønsted acidity can develop acidity high enough to catalyze the hydrocracking of *n*-hexadecane and FT waxes when Pt was introduced. Furthermore, the introduction of MoO_3 and WO_3 boost the number of sites with mild acidity. The effect of mild acidity together with a high Pt dispersion and the presence of specific pore sizes have allowed the preparation of a catalyst for hydrocracking of FT waxes with superior diesel selectivity, producing a product with excellent ignition and cold flow properties.

Experimental Section

Catalysts. The commercially available support material Siral40 and the Siral75 support material which is noncommercial were supplied by Sasol Germany GmbH (formerly Condea Chemie GmbH). The Siral material is manufactured according to procedures describe in the patent literature.[13] Aluminum alkoxides with a carbon distribution of C_2 to C_{20+} were thereby hydrolyzed with deionized water and stirred for approximately 45 min. The aqueous alumina suspension separating from the alcohols was then mixed with orthosicilic acid deionized by means of an ion exchanger in a total quantity of 3% by weight. The solid suspension obtained was dried with a spray drier at 300−600 °C. The amorphous support material Siral40 contained 40 mass % silica and 60 mass % alumina while the Siral75 material contained 75 mass % silica and 25 mass % alumina. The catalytic performance of the Siral supported catalysts was

[†] Tel.: +27 16 960-3830. Fax: +27 11 522-3975. E-mail: dieter.leckel@sasol.com.

10.1021/ie0700922 CCC: $37.00
Published on Web 04/18/2007

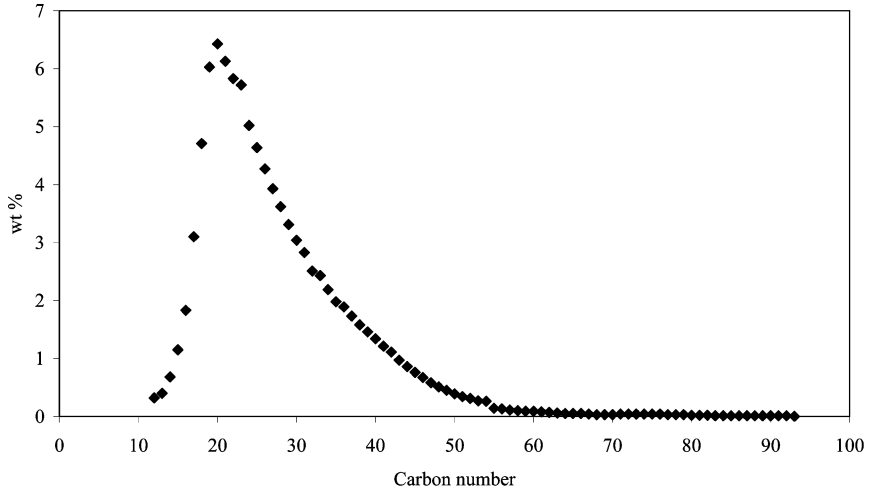

Figure 1. Carbon number distribution of Fischer−Tropsch wax used in the study.

compared to a randomly selected commercial state of the art sulfided hydrocracking catalyst which was also supported on amorphous silica−alumina (T40). It must be noted that alternative catalysts could perform differently than the one chosen for the study. Detailed analyses of the commercial catalyst were not possible due to a secrecy agreement signed with the catalyst supplier.

Metal Impregnation Procedure and Catalyst Activation.[14] The catalysts were prepared by incipient wetness impregnation. Thus, the Siral support material (1.5 mm extrudates, 100 g) was calcined in air by applying a heating rate from ambient to 500 °C at 2 °C/min. The temperature was kept at 500 °C for 3 h. The calcined material was then impregnated with a solution of ammonium metatungstate ($(NH_4)_6H_2W_{12}O_{40}\cdot xH_2O$, Fluka, ≥85% WO_3) sufficient to load 3.0 mass % WO_3. The material was again calcined by applying a heating rate of 2 °C/min from ambient to 500 °C and held at the latter temperature for 4 h. Thereafter, 100 g of the calcined material was subsequently impregnated with an aqueous solution of $[Pt(NH_3)_4](NO_3)_2$ (99.995% purity, Sigma Aldrich) containing the required amount to obtain 0.30 mass % of platinum in the final catalyst. The catalytic material was calcined once more at 500 °C in air for 4 h. Following this, the catalyst was activated in situ by first drying the material at 120 °C for 2 h in nitrogen (0.5 L/min) and subsequently conducting the reduction at 400 °C for 3 h using a hydrogen flow of 1.7 L/min (heating rate of 25 °C/h from 120 to 400 °C). The catalysts modified with MoO_3 were prepared accordingly using the precursor ammonium heptamolybdate $[(NH_4)_6\ Mo_7O_{24}\cdot 4H_2O]$ purchased from Fluka (purity >99%). All Pt-containing catalysts prepared had a metal content of 0.30% by mass.

Reactor System. An isothermally operated microscale fixed-bed reactor with 15 mm inner diameter and 600 mm length was used in down flow mode for the hydrocracking reactions. For the hydrocracking experiments 30 mL of 1.5 mm extrudated catalyst was loaded in the middle section of the reactor tube. Silicon carbide (SiC, 0.5 mm) was used to fill the voids between the catalyst particles to avoid channeling. Inert packing (glass beads) above the catalyst bed was used to preheat the feed up to the reaction temperature. The reactor was heated electrically by three independently controlled heater elements placed along the reactor tube. Liquid feed and hydrogen entered concurrently from the top of the reactor. The gas flow was measured with a wet gas meter. The gas and liquid products were separated in the last section of the reactor setup. The liquid product was collected in a catch pot and the gaseous light hydrocarbons were passed through a cooling coil at 0 °C. This condensed liquid was collected in a second gas liquid separator. A gas sampling point was installed on the low-pressure side of the reactor system.

Procedure. Hydrocracking catalyst activity was monitored by drawing product samples from the reactor after steady-state conditions were reached after each change of reactor conditions, typically after 24 h for the tests using *n*-hexadecane and a 72 h period for the wax hydrocracking experiments. The following 8 h period was then used to collect a representative sample for product analysis. Mass balances of 98−102% were achieved with collection of the tail gas, condensed lighter hydrocarbons, and liquid products from the reactor stream. Condensed light hydrocarbons were kept refrigerated prior to analysis. Conversion in hexadecane hydrocracking is defined as conversion based on the *n*-C_{16} carbon number decrease. The conversion for hydrocracking the FT wax (denoted C_{23+} conversion) is understood to be true conversion since, according to the definition used, naphtha and diesel already present in the feed are corrected for. The hydrocracking conversion ("true" conversion) is defined as described in eq 1.

$$\%\ C_{23+}\ \text{Conversion} = \left(\frac{\text{wt \% } C_{23+}\ \text{in Feed} - \text{wt \% } C_{23+}\ \text{in Product}}{\text{wt \% } C_{23+}\ \text{in Feed}}\right) \times 100 \quad (1)$$

Operating Conditions. Hydrocracking of *n*-hexadecane was performed in the temperature range of 340−380 °C. A hydrogen pressure of 5.0 MPa was applied. The liquid hourly space velocity (LHSV) was kept at 1.5 h^{-1} and the hydrogen-to-liquid ratio was adjusted to 1000:1 m^3/m^3. Experiments were performed downflow in once-through mode. Hydrocracking of FT wax was performed in the same temperature range and hydrogen-to-feed ratio; however, a higher pressure of 7.0 MPa and a LHSV of 1.0 h^{-1} was applied.

Feed. The *n*-hexadecane (99% purity) was obtained from Aldrich and used as received. The low-temperature FT wax was obtained from the Sasol 1 plant in Sasolburg, South Africa, and had a carbon number distribution ranging from C_{13} to C_{80}, peaking at carbon number C_{21} (see Figure 1).

Catalyst Characterization. The elemental composition and metal loading were determined by inductive coupled plasma (ICP). The BET surface area, the average pore volume, and the average pore diameter were measured by the BJH desorption method using N_2 physisorption with a Micromeritics TriStar

3000 analyzer. Instrument control and calculations were done using the TriStar software which is consistent according to ASTM methods D3663-99, D4222-98, and D4641-94. Average pore size was calculated as 4V/A (V: pore volume; A: surface area). The noble metal dispersion was determined by CO chemisorption with an ASAP 2010C (V3.01H).

FTIR data of adsorbed pyridine were used to determine Lewis and Brønsted acidity. The concentration of the acid sites was determined from the intensities of the bands at 1545 and 1452 cm^{-1} by integration. A Bruker Vector 22 spectrophotometer fitted with AABSPEC #2000-A multimode system transmittance cell was used for the FTIR study. AABSPEC #2000-A is an all-metal high-vacuum cell fitted with KBr windows. This cell is design to operate at vacuum up to 10^{-8} Torr and temperatures of up to 900 °C. Opus NT software from Bruker was used to operate the spectrophotometer. The instrument was operated in the absorption mode at a resolution of 4 cm^{-1} and collected 128 scans per spectrum. Self-supporting wafers were prepared using 20 mg of each sample. The wafer was degassed at 500 °C under vacuum (2.3×10^{-5} Torr) for 12 h. A background spectrum of air was collected prior to loading the sample in the cell. Pyridine, dried using molecular sieve 3 Å, was adsorbed at 100 °C and allowed to equilibrate for 12 min. Excess pyridine was evacuated at 100 °C for 1 h; this also allowed for the removal of the weakly physisorbed pyridine molecules. The sample was then cooled to room temperature prior to collecting the sample spectrum.

Product Analyses. The gaseous and liquid reactor products were analyzed by a Hewlett-Packard HP 5890 gas chromatograph fitted with FID detection using a 50 m × 0.2 mm × 0.5 μm PONA column.

Cloud Point and Cetane Index. Determination of the cloud point was based on the ASTM D 2500 method. Reproducibility was within 2 °C. Cetane numbers above the value of 70, determined by the ASTM method D 613-95, have a reproducibility of only 6−7 cetane numbers and about 2 L of diesel is required for the determination. More convenient methods requiring only small sample volumes and giving good relations for calculating cetane numbers based on proton NMR analyses are described by O'Connor et al.[15] and published in SAE 892073[16] and SAE 861521.[17] The latter publications give correlations including factors for aromatic as well as for olefinic protons. All three methods were compared to cetane numbers from the literature[18] and ASTM method D-613. The method described in SAE 861521 gave the best correlations and was therefore subsequently used for the calculation of the cetane index in our investigations.

Results and Discussion

Physicochemical Catalyst Characterization. In Table 1 physicochemical properties of the catalyst supports and the hydrocracking catalysts prepared thereof are presented. The highest surface area (498 $m^2\ g^{-1}$) was measured for the Siral40 support material followed by the Siral75 material (402 $m^2\ g^{-1}$). After the impregnation of the Siral40 support material with platinum, the surface area decreased significantly (332 $m^2\ g^{-1}$). This is not due to a pore blockage by the metal (notice that only 0.30 mass % of Pt is introduced), but by the collapse of some of the micropores and formation of mesopores after the second calcination. The platinum loading procedure had, however, less of an effect on the Siral75-based catalytic material where the surface area remained almost unchanged. Further modification with MoO_3 and WO_3 oxide changed the surface area of the resulting catalysts only to a minor extent. It is to be noted, however, that the final surface area of the PtW40 and PtW75 was practically the same. Meanwhile, and after the consecutive calcinations, the mean pore diameter of the Siral40-based catalysts increased from 5.9 nm (Siral40) to 9.3 nm for the catalyst PtW40, while the opposite effect was observed for the Siral75-based catalysts. The mean pore diameter decreased from 5.6 nm for the original Siral75 support material to 3.4 for the catalyst PtW75. It is at present unclear which parameter is responsible for this pore size effect. Further studies are necessary to understand the increase in mean pore diameter for the Siral40-based material and the decrease for the Siral75-based material. The pore size distribution of the PtW40 and PtW75 are presented in Figure 2. The platinum dispersion of PtW75 (75.7%) was found to be significantly higher than that of the PtW40 catalyst (36.1%), which could be due to the presence of micropores in the former catalyst. This is most likely an indication that Pt crystallites reside within the micropores of the Siral75 support, which is not the case with PtW40 which does not have micropores.

Table 1. Physicochemical Properties of the Catalysts Based on Siral Support Material (Pore Volume and Pt Dispersion Determined Only for PtW40 and PtW75)

Siral catalyst	BET surface area ($m^2\ g^{-1}$)	mean pore diameter (nm)	pore volume ($cm^3\ g^{-1}$)	Pt dispersion (%)
Siral40	498	5.9		
Pt40	332	8.0		
PtMo40	304	8.4		
PtW40	318	9.3	0.73	36.1
Siral75	402	5.6		
Pt75	407	3.2		
PtMo75	342	3.5		
PtW75	357	3.4	0.30	75.7

FTIR Spectroscopy Using Pyridine as a Probe Molecule for Acidity Characterization. The assignment of the bands in the FTIR spectra was done according to the literature.[8,19−21] The band located in the 1540−1550 cm^{-1} region and the band at 1639−1640 cm^{-1} was attributed to pyridinium ions, providing evidence of Brønsted acidity on the surface. The band at 1452−1455 cm^{-1} is attributed to pyridine coordinated at Lewis acid sites (coordinatively unsaturated Al^{3+} ions).

Figure 3 presents the FTIR pyridine adsorption spectra in the 1400−1700 cm^{-1} region of the Siral40 material (spectrum A) and the prepared catalysts thereof (spectra B, C, and D), meaning material containing Pt, WO_3, and MoO_3. Spectrum (A) shows predominant bands at 1619 and 1452 cm^{-1}, which can be ascribed to Lewis-bonded pyridine. The presence of bands at 1548 and 1639 cm^{-1} indicate the presence of Brønsted acid sites.

The spectrum looks very similar to cohydrolyzed silica−alumina supported commercial cracking catalysts.[22] Adding platinum to the catalyst support (Catalyst D) changes the spectrum significantly. The band at 1548 cm^{-1}, which is the most representative of the presence of Brønsted acid sites, disappeared almost completely and is not recovered after modifying the catalyst with MoO_3 or WO_3 (spectra B and C).

In Figure 4 the spectrum (A) represents the FTIR pyridine adsorption spectra of Siral75, displaying significant bands at 1597 and 1446 cm^{-1}, which are typical for an infrared spectrum of pyridine on pure silica producing only hydrogen-bonded pyridine (vibrations denoted 8a and 19b).[8] Virtually no Brønsted acidity (1548 and 1640 cm^{-1}), but only some Lewis acidity was detected. This confirms the results of Daniell et al.[12] in their low-temperature FTIR study using CO absorption that infer the absence of Brønsted acidity on Siral60−80 samples. Contrary

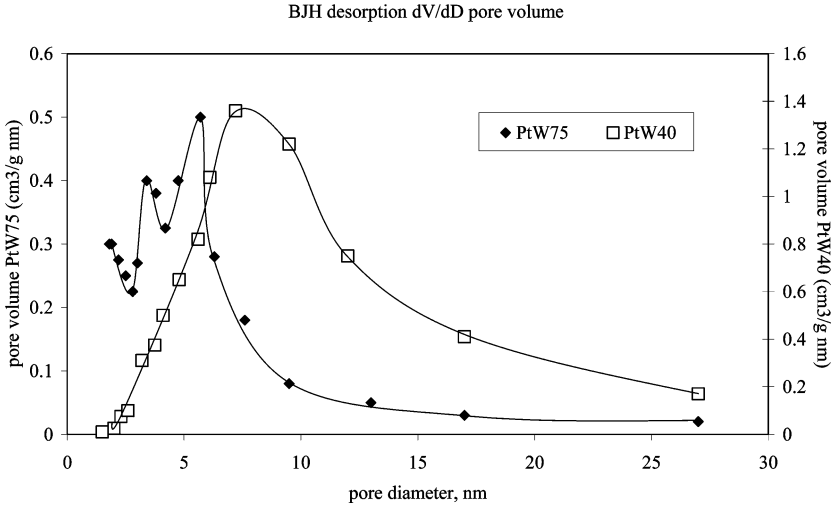

Figure 2. Pore size distribution of the PtW75 and PtW40 hydrocracking catalyst.

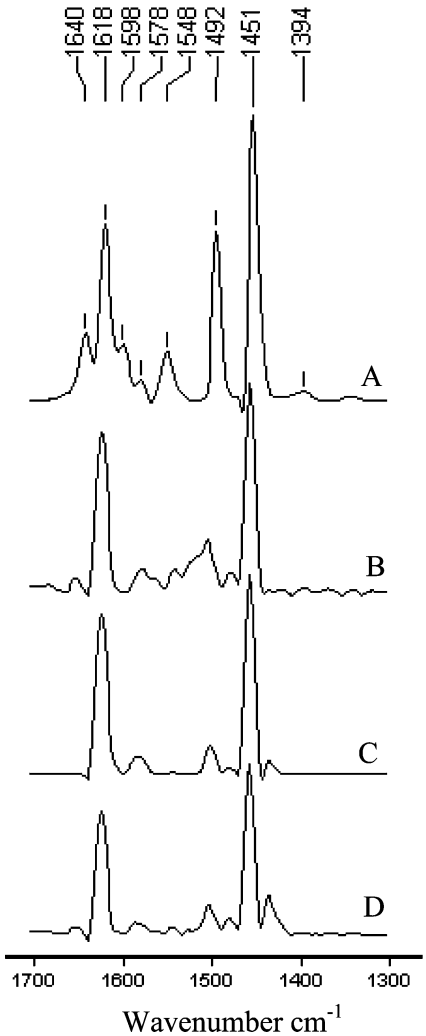

Figure 3. FTIR pyridine adsorption spectra of (A) Siral40, (B) Pt40, (C) PtW40, and (D) PtMo40.

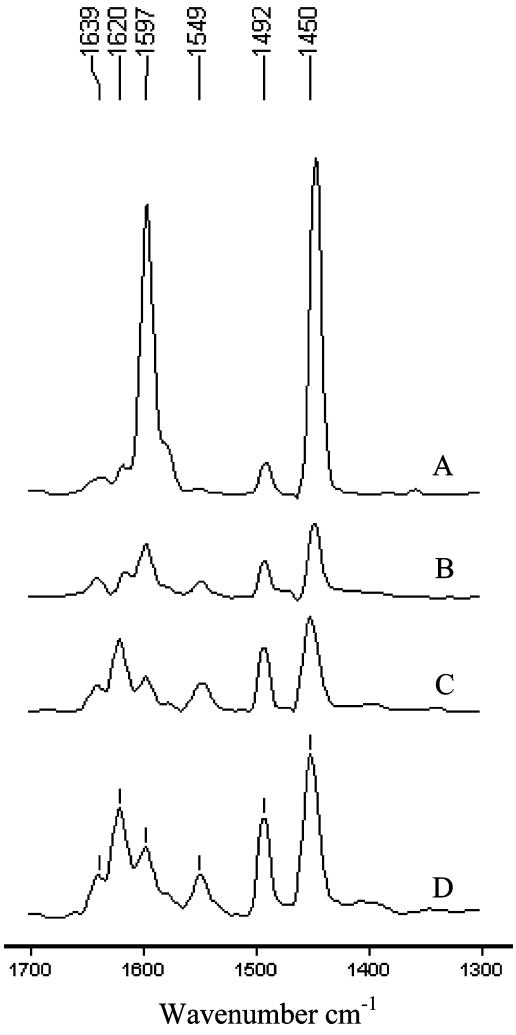

Figure 4. FTIR pyridine adsorption spectra of (A) Siral75, (B) Pt75, (C) PtW75, and (D) PtMo75.

to Siral40 (see Figure 3), the addition of platinum on the Siral75 material (spectrum D) produces an increase in Brønsted and a decrease in Lewis acidity. The subsequent modification with MoO_3 and WO_3 increased the amount of Brønsted sites. Quantitative information (concentration of Brønsted and Lewis acid sites) was obtained by integrating the area under the relevant peaks using the baseline as a straight line joining the frequency limits of the peak envelope, and the results are reported in Table 2.

Larson et al.[23] attributed the decrease in catalyst acidity in their work on the effects of platinum area and surface acidity on the hydrocracking activity of furnace oil to the adsorption of platinum on acid sites, specifically strong acid sites. Platinum addition (especially in the range of low Pt loadings) induced

Table 2. Quantitative Information (Concentration of Brønsted and Lewis Acid Sites) Obtained by Integrating the Area under the Relevant Peaks 1548 cm^{-1} and 1452 cm^{-1}

Siral catalyst	concn of Brønsted acid sites (10^{-3} mg^{-1})	concn of Lewis acid sites (10^{-3} mg^{-1})
Siral40	18	117
Pt40	2.1	94
PtMo40	9.2	99
PtW40	5.4	80
75		40
Pt75	10	30
PtMo75	15	70
PtW75	14	36

an increase in acidity on the catalyst which was also observed in our study for the addition of platinum to the Siral75 material.

If we assume, according to Larson et al.,[23] that platinum adsorbs on the acid sites and specifically the acid sites of larger strength, then impregnation of the Siral40 support, having the higher Brønsted acidity compared to Siral75 (Table 2), would result in the concentration (agglomeration) of Pt at these acid sites. The acidity of the catalyst would decrease since the acid sites are more or less blanketed by the metal, and a lower dispersion of the Pt would also be observed. This was indeed observed (Table 1 and Table 2).

Impregnation of a support with virtually no Brønsted acidity (as determined by pyridine adsorption, see Figure 4 and Table 2), such as Siral75, would on the other hand result in a higher metal dispersion since there are no areas of preferred adsorbance and the metal is randomly distributed. However, the reason for the increasing acidity of the Pt-loaded Siral75 material is not quite apparent.

Hydrocracking Activity Using *n*-Hexadecane as FT Wax Model Compound. Figure 5 presents the hexadecane conversion for the Siral40 and Siral75 supported catalysts at increasing operating temperature and otherwise constant reaction conditions. Conversion is based on the decrease in *n*-C_{16} carbon number. In general, conversion increases with increasing temperature and the lowest hydrocracking activity was observed for the Siral40-based catalysts. The platinum-impregnated Siral75 supported catalyst showed thereby a 70% higher conversion than the Siral40-based catalyst at the lower temperatures (340−345 °C) and a 40% higher conversion at the temperature of 360 °C. The molybdenum and platinum modified catalysts showed the same trends; however, at 360 °C the percentage of conversion was only 20% higher compared to that of the Siral40-based catalyst. Owing to the larger number of acid sites, the Siral75-based catalyst required a much lower temperature to attain a given *n*-C_{16} conversion. To obtain the 70% conversion level, the PtW40 needed a temperature of 360 °C while the PtW75 achieved this conversion already at 340 °C. As noticed from Figure 5, the relationship between temperature and conversion is similar for the Pt40, PtW40, and Pt75 catalysts. A nearly identical slope of the straight line is observed for the temperature range investigated. However, temperature affects the hydrocracking activity of the PtW75 catalyst not as significantly; the slope of the straight line is not as steep. Temperature has generally an indirect effect on the product distribution by shifting the vapor−liquid equilibrium composition and lowering the residence time of the gas fraction.

Apparent kinetic rate constants for hydrocracking were calculated for each catalyst at 360 °C considering a first-order kinetic expression for *n*-hexadecane, while the partial pressure of H_2 remained practically constant (Figure 6). When the apparent kinetic rate constants are plotted versus the concentration of Brønsted acid sites given in Table 2, a reasonable linear correlation is obtained. It is to be noted, though, that the rate constants determined for the Siral75 supported catalysts were higher than those for the Siral40 catalysts. These results indicate in first approximation that mainly the Brønsted acid sites generated influence the final hydrocracking activity of the catalysts.

However, we tentatively suggest that in addition to Brønsted acidity the higher Pt dispersion on the Siral75 compared to the Siral40 samples are responsible for the better hydrocracking performance and bifunctionality in the case of the former catalysts. In fact, the better dispersion of the noble metal decreases the distance between the isomerization and dehydrogenation sites and favors the formation of carbenium ions on the Brønsted site close to the metal site where the olefin is formed. Taking this into consideration, we can expect the Siral75-derived materials to be better bifunctional catalysts than those derived from Siral40. Then, if this is true, a lower selectivity to methane should be observed in the products when using the Siral75 catalysts. Results from Figure 7 show that the $C_1 + C_2$ yield is slightly higher for Siral40-based catalyst and for the commercial catalyst than for PtW75 catalyst. Figure 8 shows furthermore that the selectivity to products with different carbon number is shifted toward longer chains in the case of the Siral75-derived sample compared to the Siral40 catalytic material.

Hydrocracking Selectivity. In the case of the wax hydrocracking, overcracking should be minimized to achieve maximum diesel yield. Meanwhile, a good balance between monobranched and normal alkanes is desired to optimize cetane number and cloud points in the diesel formed. All the above requirements could be accomplished through the design of bifunctional catalysts containing mild acidity, high metal dispersion, and a pore size distribution where most of the pores reside in the range of 3.0−7.0 nm.[24] If the above requirements are accomplished, then one could expect the following: (a) low ($C_1 + C_2$) gas formation, (b) a Gaussian curve for products[25] with the maximum located in the C_8 carbon range when cracking hexadecane, and (c) a maximum yield of liquid products at conversion of 80% or higher.

In our work, we have compared the selectivity behavior outlined above in (a), (b), and (c) for PtW40 and PtW75 and the results are compared with those of a bifunctional hydrocracking catalyst based on a amorphous silica−alumina (T40) and used commercially for hydrocracking. Results from Figure 7 showed a higher yield for the ($C_1 + C_2$) fraction (dry gas) for the Siral40-based and the commercial catalyst when compared at a 55% level of conversion. Specifically, the Pt75 catalyst showed the lowest dry gas formation. Figure 8 shows the carbon number distribution for the liquid products when *n*-hexadecane was cracked at 55% conversion and it clearly indicates a closer behavior to ideal hydrocracking[6,25,26] for the Siral-based catalysts compared to the commercial catalyst. A maximum at C_8 is obtained for the products hydrocracked with the Siral-based catalysts with progressively lower concentrations of hydrocarbons more distant from this carbon number. The commercial catalyst showed a higher cracking selectivity to the shorter chain molecules such as C_5 to C_7 and a lower selectivity for the higher carbon numbers. This indicates that the commercial catalyst promotes secondary reactions while the Siral-based catalysts support primary hydrocracking reactions.

Unfortunately, data at higher conversions were not available, but if we consider the results from Figures 7 and 8, we can

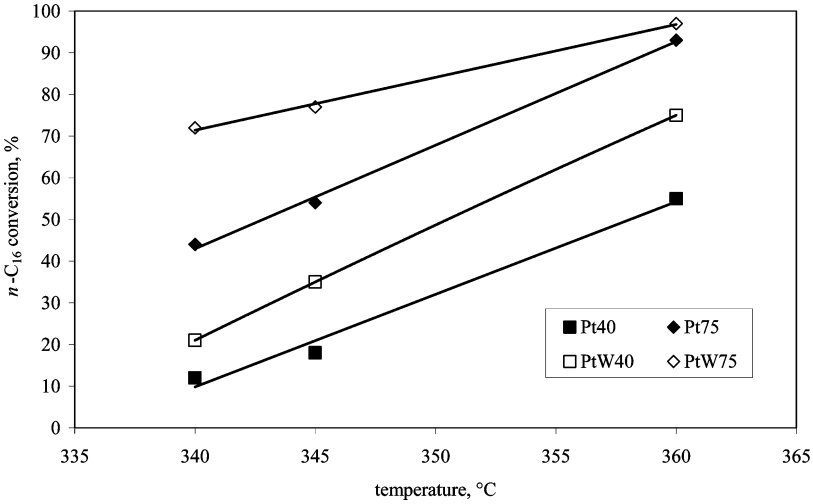

Figure 5. Percentage conversion obtained for the hydrocracking of *n*-C_{16} at increasing temperature using the Siral40- and Siral75-based catalysts.

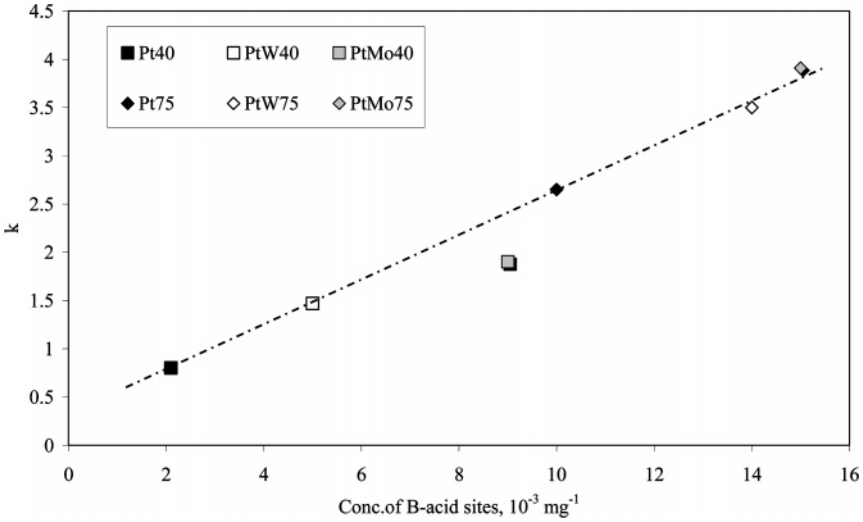

Figure 6. First-order rate constant *k* for the hydrocracking of *n*-hexadecane with Siral-based catalysts plotted over the concentration of Brønsted acid sites.

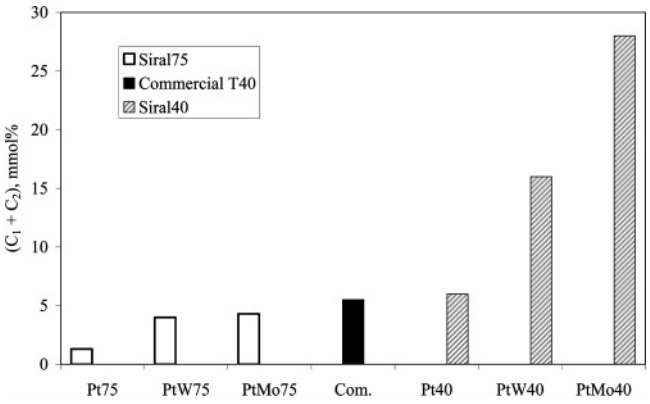

Figure 7. Comparison of ($C_1 + C_2$) yields produced during hydrocracking of *n*-hexadecane with the Siral-based and the commercial catalyst at 55% conversion.

forecast, in a first approximation, that the Siral-based catalysts, especially the Siral75-based catalysts, should compare very well, if not better, with the commercial catalyst when used for hydrocracking Fischer−Tropsch (FT) waxes.

Hydrocracking FT Waxes. Since the PtW75 catalyst provided our requirements for mild acidity, large Pt dispersion, and pore diameters in the range of 3.0−7.0 nm and, furthermore, showed good hydrocracking behavior when using hexadecane as a test molecule, we decided to investigate its selectivity for producing diesel and naphtha by hydrocracking FT waxes. The results are compared with those obtained with the commercial T40 and the PtW40 catalyst. Figure 9 clearly shows that the yield of diesel is larger and the yield of naphtha is lower for the PtW75 catalyst than that for the commercial catalyst at higher levels of conversion. The PtW40 showed the worst FT wax hydrocracking performance, producing the lowest diesel and the highest naphtha yields. Moreover, the cloud point and cetane index for the diesel produced by the PtW75 are −11 °C and 77, respectively, while they are −8 °C and 79 for the commercial catalyst. This indicates that the Pt- and W-containing catalyst based on amorphous aluminosilicate with high silica content (Siral75) is able to produce a diesel with excellent fuel properties. At the same time a much higher diesel fraction is obtained at higher conversions than with the PtW40 and commercial catalyst, the latter being specifically designed for diesel-selective hydrocracking.

Platinum dispersion and also the pore structure of the catalyst seem to affect the diesel selectivity, with larger proportions of mesopores being detrimental to diesel formation at high conversions (as observed for the PtW40, see Figures 2 and 9). Overcracking of the wax specifically at the higher conversion levels is not observed with the PtW75 catalyst rather than with the PtW40 catalyst, the latter producing more material in the naphtha range. This is the effect of the lower metal distribution of the PtW40 catalyst, leading to the consequence that the

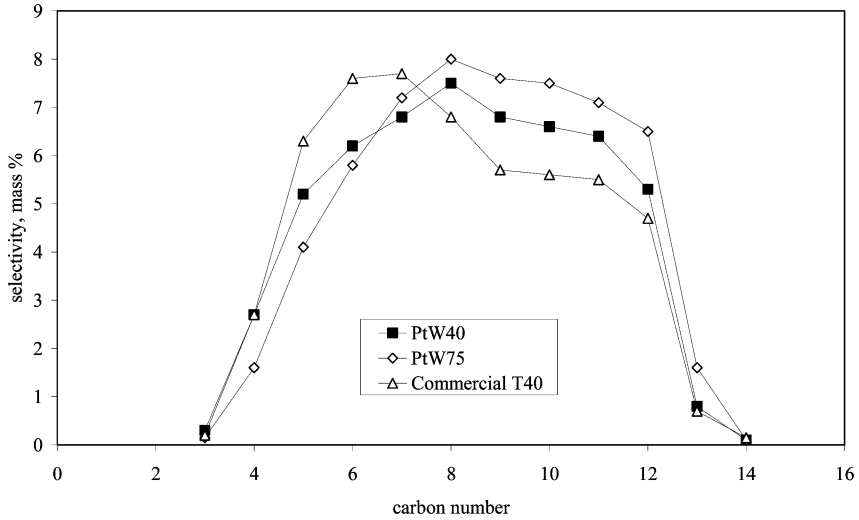

Figure 8. Comparison of carbon number distribution produced during hydrocracking of *n*-hexadecane with the Siral-based and the commercial catalyst T40 at 55% conversion.

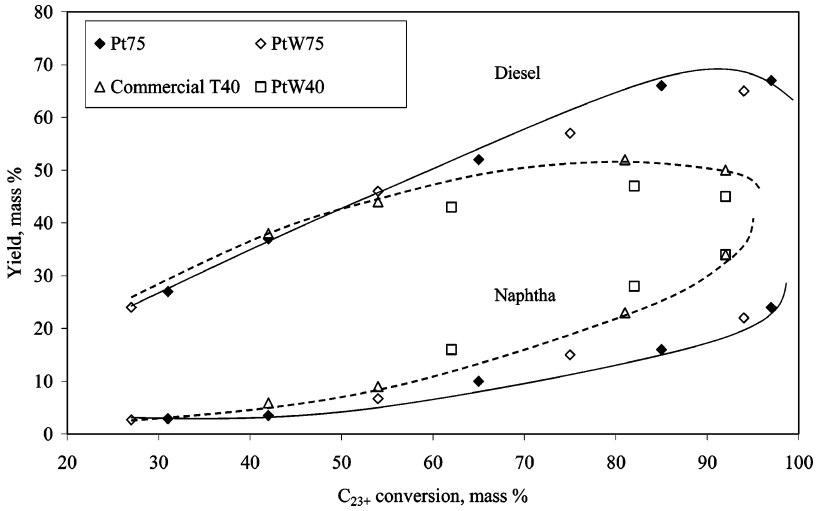

Figure 9. Comparison of naphtha and diesel yields during hydrocracking of LTFT wax with the Siral75-based catalysts and the commercial catalyst.

unsaturated alkene intermediates are rather subjected to further acid-catalyzed skeletal rearrangements and secondary cracking reactions than being hydrogenated at a metal site.

Conclusions

Amorphous silica−aluminas formed by alumina obtained from aluminum alkoxides and "sililated" with orthosicilic acid have shown Brønsted acidity when the silica content is 40% (Siral40), while no Brønsted acidity was observed when the silica content was 75% (Siral75).

The introduction of Pt or Pt and W generates Brønsted acidity on Siral75 (PtW75) giving higher numbers of acid sites than in the case of Siral40 (PtW40).

Both higher acidity and metal dispersion in the PtW75 resulted in a more active and selective catalyst for hydrocracking of *n*-hexadecane.

Results obtained with PtW75 compare very well or even improve those of a commercial hydrocracking catalyst when using *n*-hexadecane as a test reaction, and this conclusion is confirmed when hydrocracking FT waxes, showing an improved performance in the case of the PtW75.

The catalytic behavior cannot be related to the Pt dispersion alone. The data indicate that the pore structure of the support has an influence on catalyst selectivity and it seems that larger mesopores are detrimental to the formation of diesel at high conversions.

Further studies are necessary to understand the fundamental effects of Pt loading only and additional MoO_3 and WO_3 loading on the hydrocracking performance of the catalysts.

Acknowledgment

The technical contributions of M. Liwanga-Ehumbu and the analytical support of the Materials Characterization Group are gratefully acknowledged. The author appreciates in particular the constructive discussions with Professor Avelino Corma. All work was performed at Sasol Technology Research and Development and permission to publish this work is appreciated.

Literature Cited

(1) Leckel, D. *Energy Fuels* **2005**, *19*, 1795.

(2) Zhang, S.; Zhang, Y.; Tierney, J. W.; Wender, I. *Fuel Process. Technol.* **2001**, *69*, 59.

(3) Sie, S. T.; Senden, M. M. G.; Van Wechem, H. M. H. *Catal. Today* **1991**, *8*, 371.

(4) Leckel, D.; Liwanga-Ehumbu, M. *Energy Fuels* **2006**, *20*, 2330.

(5) Scherzer, J.; Gruia, A. *Hydrocracking Science and Technology*; Marcel Dekker: New York, 1996.

(6) Coonradt, H. L.; Garwood, W. E. *Ind. Eng. Chem. Process Des. Dev.* **1964**, *3*, 38.

(7) Corma, A.; Martínez, S.; Pergher, S.; Peratello, S.; Perego, G.; Bellussi, G. *Appl. Catal. A* **1997**, *152*, 177.

(8) Nilsen, B. P.; Onuferko, J. H.; Gates, B. C. *Ind. Eng. Chem. Fundam.* **1986**, *25*, 337.

(9) Iengo, P.; Di Serio, M.; Solinas, V.; Gazzoli, D.; Salvio, G.; Santacesaria, E. *Appl. Catal. A* **1998**, *170*, 225.

(10) Buonomo, F.; Fattore, V.; Notari, B. U.S. Patent 4,013,589, March 22, 1977. Buonomo, F.; Fattore, V.; Notari, B. U.S. Patent 4,013,590, March 22, 1977. Manara, G.; Fattore V.; Notari, B. U.S. Patent 4,038,337, July 26, 1977. All patents were assigned to Snamprogetti SpA.

(11) Niwa, M.; Katada, N.; Murakami, Y. *J. Phys. Chem.* **1990**, *94*, 6441.

(12) Daniell, W.; Schubert, U.; Glöckler, R.; Meyer, A.; Noweck, K.; Knözinger, H. *Appl. Catal. A* **2000**, *196*, 247.

(13) Meyer, A.; Noweck, K.; Reichenauer, A.; Schimanski, J. U.S. 5,-045,519, Sept 3, 1991. Assigned to Condea Chemie GmbH.

(14) Liwanga-Ehumbu, A-M.; Visagie, J. L.; Leckel, D. O. GB 2,380,953, Apr 23, 2003. U.S. Patent 2003/0173253 A1, Sept. 18, 2003; WO 01/90280 A2, Nov. 29, 2001; AU 200168761 B2, Patent No. 782723, May 24, 2001. All patents assigned to Sasol Technology.

(15) O'Connor, C. T.; Forrester, R. D.; Scurrell, M. S. *Fuel* **1992**, *71*, 1323−1327.

(16) Gulder, O. L.; Glavincevski, B.; Kallio, N. N. *A Rapid Cetane Number Prediction Method for Petroleum Liquids and Pure Hydrocarbons using Proton NMR*; SAE Technical Paper Series 892073; SAE: Warrendale, PA, 1989.

(17) Bailey, B. K.; Russell, J. A.; Wimer, W. W.; Buckingham, J. P. *Cetane Number Prediction from Proton-Type Distribution and Relative Hydrogen Population*; SAE Technical Paper Series 861521; SAE: Warrendale, PA, 1986.

(18) *Technical Data on Fuel*, *7th Edition*; Rose, J. W., Cooper, J. R., Eds.; Wiley: New York, 1977.

(19) Basila, M. R.; Kantner, T. R.; Rhee, K. H. *J. Phys. Chem.* **1964**, *68*, 3197.

(20) Bourne, K. H.; Cannings, F. R.; Pithehly, R. C. *J. Phys. Chem.* **1970**, *74*, 2197.

(21) Parry, E. P. *J. Catal.* **1963**, *2*, 371.

(22) Bevilacqua, M.; Montanari, T.; Finocchio, E.; Busca G. *Catal. Today* **2006**, *116*, 132.

(23) Larson, O. A.; MacIver, D. S.; Tobin, H. H.; Flinn, R. A. *Ind. Eng. Chem. Process Des. Dev.* **1962**, *1*, 300.

(24) Espinoza, R. L.; Lawson, K. H.; Jothimurugesan, K. U.S. Patent Application 2006/0011512 A1, Jan. 19, 2006. Lawson, K. H.; Jothimurugesan, K.; Espinoza, R. L. U.S. Patent Application 2005/0274646 A1, Dec. 15, 2005. All assigned to ConocoPhillips Company.

(25) Steijns, M.; Froment, G.; Jacobs, P.; Uytterhoeven, J.; Weitkamp, J. *Ind. Eng. Chem. Prod. Res. Dev.* **1981**, *20*, 654.

(26) Degnan, T. F.; Kennedy, C. R. *AIChE J.* **1993**, *39* (4), 607.

Received for review January 15, 2007
Revised manuscript received March 9, 2007
Accepted March 22, 2007

IE0700922